Quantization of the quasiparticle spectrum in the mixed state of d-wave superconductors

1999 J. Phys.: Condens. Matter 11 4219

(http://iopscience.iop.org/0953-8984/11/21/309)

J. Phys.: Condens. Matter **11** (1999) 4219–4229. Printed in the UK PII: S0953-8984(99)98807-0

Quantization of the quasiparticle spectrum in the mixed state of d-wave superconductors

A S Mel'nikov

Institute for Physics of Microstructures, Russian Academy of Sciences, 603600, Nizhny Novgorod, GSP-105, Russia

Received 28 October 1998, in final form 19 January 1999

Abstract. We have investigated the distinctive features of the band spectrum, eigenfunctions, and density of states (DOS) for low-lying quasiparticle excitations in the mixed state of clean d-wave superconductors ($H_{c1} \ll H \ll H_{c2}$). Our study is based on an approximate analytical solution of the Bogoliubov–de Gennes equations for quasiparticles with momenta close to gap node directions. Both the quantized energy spectrum and the spatially averaged residual DOS are shown to depend fundamentally on the vortex lattice geometry.

1. Introduction

Recently a great deal of attention has been devoted to the nature of the quasiparticle states in isolated vortices and vortex lattices in superconductors with anisotropic pairing. This problem is of considerable importance since low-energy quasiparticle excitations impact on various static and dynamic properties of the mixed state at low temperatures. These investigations were stimulated by a large number of experiments which provide good evidence for d-wave symmetry of the order parameter in high-temperature superconductors (see [1] and references therein). For conventional s-wave superconductors the low-lying quasiparticle states are bound to the vortex cores as was first predicted by Caroli, de Gennes, and Matricon [2]. For an isolated vortex line the eigenvalues for these localized states may be written as follows: $E_\mu \sim \mu\Delta/(k_F\xi)$, where Δ is the gap value far from the vortex axis, ξ is the coherence length at $T = 0$, k_F is the Fermi momentum, and the angular momentum quantum number μ is half an odd integer. Despite the number of theoretical and experimental investigations a clear physical picture of the electronic structure of the mixed state in d-wave systems is still lacking. In contrast to that for conventional superconductors, the density of states (DOS) at low energies in d-wave systems is dominated by contributions which come from the regions far from the vortex cores and depends essentially on the intervortex distance R_v. This unusual fact is a direct consequence of the vanishing pair potential in the directions of the gap nodes. As a result, one obtains the specific magnetic field dependence of the DOS at the Fermi level (see [3–5]), which may be experimentally identified, for instance, in specific heat [6–8] or scanning tunnelling microscope (STM) [9] measurements. It should also be emphasized that there is an important difference between the quantization of the energy spectrum in the mixed state of s- and d-wave superconductors: for s-wave systems the energy quantization and corresponding localized states exist even in a single isolated vortex line (and they are weakly influenced by the presence of neighbouring vortices at least for $R_v \gg \xi$) while for the d-wave case the low-lying energy spectrum may be quantized only due to the finite intervortex distance

0953-8984/99/214219+11$19.50

(see [10–14]). The latter conclusion is proved by the numerical solution of the Bogoliubov–de Gennes (BdG) equations [15] which shows that there are no truly localized states for a single isolated vortex in a pure d-wave superconductor.

The simplest theoretical description of the excitation spectrum is based on the semiclassical approach which takes account of the Doppler shift of the quasiparticle energy due to the local superfluid velocity $\boldsymbol{V}_s$:

$$\varepsilon(\boldsymbol{k}, \boldsymbol{r}) = \pm\sqrt{\hbar^2 V_F^2 (k - k_F)^2 + \Delta^2(\boldsymbol{k})} + \hbar \boldsymbol{k} \cdot \boldsymbol{V}_s(\boldsymbol{r}) \tag{1}$$

where V_F is the Fermi velocity. Hereafter we assume the Fermi surface to be two dimensional, which is appropriate to high-T_c superconductors, and take the gap function in the form $\Delta_d = \Delta_0 k_x k_y / k_F^2$ (the x-axis is taken along the [110] crystal direction and thus makes an angle $\pi/4$ with the a-axis of the CuO_2 planes). We restrict ourselves to the study of a vortex lattice under a magnetic field applied parallel to the c-axis and, as a consequence, the vector $\boldsymbol{V}_s$ is a periodic function of x, y with the periodicity of the vortex lattice. One can separate two length scales for quasiparticle wave functions: an atomic length scale k_F^{-1} and a characteristic wavelength with a slowly varying envelope, l. The semiclassical procedure is in general correct when the order parameter and superfluid velocity are modulated on a scale $\Lambda \gg l$. For s-wave superconductors we have $l \sim \xi$ (the minimum spatial extent of wave packets made with excitations (1)) and, as a result, the semiclassical approach fails only for the vortex core region. For d-wave systems the l-value appears to be angle dependent. In the homogeneous case the spectrum for the low-lying excitations which are close to one of the gap nodes (which corresponds, e.g., to the point $\boldsymbol{k} = (k_F, 0)$) has the form

$$\varepsilon(\boldsymbol{k}) \simeq \pm\Delta_0\sqrt{\xi^2 (k - k_f)^2 + k_y^2 / k_F^2} \tag{2}$$

where $\xi = \hbar V_F / \Delta_0$. The typical momenta in the x-direction are $q_x \sim \varepsilon/(\Delta_0 \xi)$ and the corresponding wavelength is of the order $l_x \sim \Delta_0 \xi / \varepsilon$. Comparing the l_x-value with the intervortex distance R_v (the characteristic length of the superfluid velocity variation), one can expect the semiclassical approach based on the expression (1) to fail for low energies $\varepsilon \lesssim \Delta_0 \xi / R_v$. In this case we may assume that the effective potential $\hbar \boldsymbol{k} \cdot \boldsymbol{V}_s(\boldsymbol{r})$ in equation (1) should be averaged over the distances $\sim l_x$ in the x-direction (the validity of these qualitative arguments will be proved below). To analyse the problem beyond the semiclassical approach one must use the more powerful methods based on either the BdG equations or Green's-function techniques (which are equivalent for clean superconductors). The quasiclassical limit ($k_F \xi \gg 1$) of these theories is known to be represented by the Andreev and Eilenberger equations, respectively. Within these models one should solve the one-dimensional quantum mechanical problem for the particle motion along the quasiclassical trajectory which is characterized by the impact parameter $b = \mu / k_F$ and the angle θ in the x–y plane [3, 10–13, 16, 17]. Using the Bohr–Sommerfeld quantization rule for the angular momentum $\mu(\theta, \varepsilon)$ one can in principle determine the true quantum levels (see [10–13]). For the d-wave case the main difficulty is connected with the description of quasiclassical trajectories which make an angle $\theta < \xi / R_v$ with the gap node directions. For this angular domain the extension of the wave function exceeds the R_v-value and quasiparticle states are sensitive to the superfluid velocity fields of all vortices even if the impact parameter is less than R_v. The correct description of these trajectories with small θ-values is of considerable importance since it is this angular interval which determines the true quantum levels according to the Bohr–Sommerfeld quantization rule. The above conclusion concerning the essential influence of the $\boldsymbol{V}_s$-field on the low-energy spectrum is also consistent with the qualitative arguments discussed in [18].

It is the purpose of this paper to report on a calculation of the quantized energy spectrum and quasiparticle eigenfunctions for various vortex lattice structures, based on an approximate analytical solution of the BdG equations for low-lying excitations with $\varepsilon \lesssim \Delta_0\xi/R_v$. Our approach provides the possibility of taking proper account of the influence of the superfluid velocity fields of all vortices in the vortex lattice on the quasiparticle motion along the trajectories almost parallel to gap node directions.

2. Basic equations

The BdG equations for spin-singlet unconventional superconductors can be written as

$$\hat{h}_0 u(\boldsymbol{r}) + \int \Delta(\boldsymbol{r}, \boldsymbol{r}')v(\boldsymbol{r}')\,\mathrm{d}\boldsymbol{r}' = \varepsilon u(\boldsymbol{r}) \tag{3}$$

$$-\hat{h}_0^* v(\boldsymbol{r}) + \int \Delta^*(\boldsymbol{r}, \boldsymbol{r}')u(\boldsymbol{r}')\,\mathrm{d}\boldsymbol{r}' = \varepsilon v(\boldsymbol{r}) \tag{4}$$

where u, v are the particlelike and holelike parts of the quasiparticle wave function. The one-particle Hamiltonian $\hat{h}_0$ in the simplest isotropic case takes the form

$$\hat{h}_0 = -\frac{\hbar^2}{2M}\left(\boldsymbol{\nabla} + \mathrm{i}\frac{\pi}{\phi_0}\boldsymbol{A}\right)^2 - E_F$$

where ϕ_0 is the flux quantum, E_F is the Fermi energy, and M is the electron effective mass. The system (3), (4) has been previously solved numerically for specific lattice models [19,20] and in the continuum limit [15,21]. To obtain the analytical solution we follow a well known procedure (see, e.g., [14,22]) and simplify the nonlocal off-diagonal terms using the condition $k_F\xi \gg 1$ (or, equivalently, $\Delta_0 \ll E_F$). In this case one can search for the solution in the form

$$u = U\exp(\mathrm{i}\boldsymbol{k}_F \cdot \boldsymbol{r}) \qquad v = V\exp(\mathrm{i}\boldsymbol{k}_F \cdot \boldsymbol{r})$$

i.e. divide out the fast oscillations on a scale k_F^{-1}. Then we rewrite $\Delta(\boldsymbol{r}, \boldsymbol{r}')$ in terms of the centre of mass $\boldsymbol{R} = (\boldsymbol{r} + \boldsymbol{r}')/2$ and relative coordinates $\boldsymbol{\rho} = \boldsymbol{r} - \boldsymbol{r}'$ and introduce the gap function as a Fourier transform with respect to $\boldsymbol{\rho}$:

$$\Delta(\boldsymbol{k}, \boldsymbol{R}) = \Delta_d(\boldsymbol{k})\Psi(\boldsymbol{R}).$$

Note that we consider the case of pure d-wave superconductivity and neglect the effects connected with the possible formation of states of mixed symmetry (with coexisting s- and d-wave or $\mathrm{d}_{x^2-y^2}$ and d_{xy} order parameter components). The function $\Psi(\boldsymbol{R}) = f\exp(\mathrm{i}\chi)$ is the d-wave order parameter used in Ginzburg–Landau theory. Let us take the two-term expansion for the gap operator:

$$\int \Delta(\boldsymbol{r}, \boldsymbol{r}')v(\boldsymbol{r}')\,\mathrm{d}\boldsymbol{r}' \simeq \mathrm{e}^{\mathrm{i}\boldsymbol{k}_F\cdot\boldsymbol{r}}\left(\Psi\Delta_d(\boldsymbol{k}_F)V - \frac{\mathrm{i}}{2}\frac{\partial\Delta_d}{\partial\boldsymbol{k}}\bigg|_{\boldsymbol{k}_F}\{\nabla, \Psi\}V\right) \tag{5}$$

where we use the notation $\{\hat{A}, \hat{B}\}$ for the anti-commutator of two operators $\hat{A}$ and $\hat{B}$. In order to obtain the Andreev equations we should keep only the first term in this expression. Obviously such an approximation is not correct, and the second term cannot be omitted when $\boldsymbol{k}_F$ is close to the gap nodes and the first term vanishes. Taking, e.g., $\boldsymbol{k}_{F1} = (k_F, 0)$ and introducing a new two-component wave function $\hat{g} = (U\exp(-\mathrm{i}\chi), V)$ (to eliminate the order parameter phase in Ψ) one obtains the equations linearized in gradient terms:

$$-\xi\hat{\sigma}_z\left(\mathrm{i}\frac{\partial}{\partial x} + \frac{\pi A_x}{\phi_0}\right)\hat{g} - \frac{\hat{\sigma}_x}{2k_F}\left\{\mathrm{i}\frac{\partial}{\partial y} + \frac{\pi A_y}{\phi_0}, f\right\}\hat{g} + \frac{M\xi}{\hbar}V_{sx}(1 + \hat{\sigma}_z)\hat{g} + \frac{Mf}{\hbar k_F}V_{sy}\hat{\sigma}_x\hat{g} = \frac{\varepsilon}{\Delta_0}\hat{g}. \tag{6}$$

Here $\hat{\sigma}_x, \hat{\sigma}_y, \hat{\sigma}_z$ are the Pauli matrices, V_{sx} and V_{sy} are the components of the superfluid velocity $\boldsymbol{V}_s = V_{sx}\boldsymbol{x}_0 + V_{sy}\boldsymbol{y}_0$, and $\boldsymbol{x}_0$, $\boldsymbol{y}_0$, $\boldsymbol{z}_0$ are the unit vectors of the coordinate system. We follow here the treatment in [14] and neglect the curvature of the Fermi surface. For an isotropic Fermi surface such an approximation is valid only for $\varepsilon \ll \Delta_0/(k_F\xi)$ (see [23, 24]). However, as mentioned in [14, 24], the range of validity of equation (6) may be even larger if the Fermi surface is somewhat flattened at the nodes.

3. Quantization of the quasiparticle spectrum in vortex lattices

At intermediate magnetic fields $H_{c1} \ll H \ll H_{c2}$ (when the intervortex distance is much smaller than the London penetration depth) we can assume $\boldsymbol{H} = -H\boldsymbol{z}_0$ to be homogeneous and take the gauge $\boldsymbol{A} = Hy\boldsymbol{x}_0$. If we neglect the terms proportional to $\boldsymbol{V}_s$ and the suppression of the order parameter in vortex cores (i.e. assume $f = 1$), then equation (6) can be solved exactly in terms of harmonic oscillator eigenfunctions. The energy spectrum has the form [14, 18]:

$$\varepsilon_N = \pm\sqrt{2\Delta_0\hbar\omega_c N}$$

where $\omega_c = eH/(Mc)$ is the cyclotron frequency and N is an integer. The latter expression, however, does not provide an adequate description of the low-energy spectrum, since the periodic potential associated with a nonzero superfluid velocity cannot be considered as a small perturbation [18]. For a vortex lattice with primitive translations $\boldsymbol{a}_1, \boldsymbol{a}_2$ the superfluid velocity may be written in the form

$$\boldsymbol{V}_s = \frac{\mathrm{i}\pi\hbar H}{M\phi_0}\sum_{\boldsymbol{b}\neq 0}\frac{[\boldsymbol{b}, \boldsymbol{z}_0]}{|\boldsymbol{b}|^2}\mathrm{e}^{\mathrm{i}\boldsymbol{b}\cdot\boldsymbol{r}} \tag{7}$$

where $[\boldsymbol{b}, \boldsymbol{z}_0]$ is the vector product of the vectors $\boldsymbol{b}$ and $\boldsymbol{z}_0$, and $\boldsymbol{b} = n\boldsymbol{b}_1 + m\boldsymbol{b}_2$, where $\boldsymbol{b}_1 = 2\pi H[\boldsymbol{a}_2, \boldsymbol{z}_0]/\phi_0$ and $\boldsymbol{b}_2 = 2\pi H[\boldsymbol{z}_0, \boldsymbol{a}_1]/\phi_0$ are the primitive translations in the reciprocal lattice; n and m run over all possible integers. As we see below, the solution of equation (6) depends strongly on the flux-lattice structure and its orientation relative to the crystal axes. Contrary to the case for the conventional isotropic superconductors (where a hexagonal flux lattice appears to be energetically favourable), for d-wave compounds previous theoretical work predicted a rich phase diagram, containing triangular, centred rectangular, and square lattices with various orientations relative to the ionic lattice, as a function of magnetic field and temperature [25–30]. In principle one should treat the problem self-consistently, i.e. calculate first the energy spectra for various vortex configurations and then find the lattice structure corresponding to the free-energy minimum.

In this paper we do not solve this self-consistent problem, and restrict ourselves to the study of energy spectra for several particular lattice structures. Let us choose one of the primitive translations (e.g. $\boldsymbol{a}_1$) to be parallel to the gap node direction $\boldsymbol{x}_0$, and consider two types of lattice: (I) $\boldsymbol{a}_1 = a\boldsymbol{x}_0$, $\boldsymbol{a}_2 = \sigma a\boldsymbol{y}_0$, $H\sigma a^2 = \phi_0$ (the rectangular lattice); (II) $\boldsymbol{a}_1 = a\boldsymbol{x}_0$, $\boldsymbol{a}_2 = a(\boldsymbol{x}_0/2 - \sigma\boldsymbol{y}_0)$, $H\sigma a^2 = \phi_0$ (vortices in the unit cell form the shape of an isosceles triangle with the base along the x-axis). Note that the centred rectangular lattices of the type II (with the parameter σ gradually changing as a function of the H- and T-values) were found to be energetically favourable for a certain region of the H–T phase diagram within a generalized London model taking account of nonlocal and nonlinear corrections to the free energy [25, 26]. We also include in our consideration the square lattice tilted by $\pi/4$ from the a-axis (type I, $\sigma = 1$) which is the most stable, at least for rather high fields and temperatures not very close to T_c according to [27–30]. Such a lattice structure (though elongated in the a-direction) is close to the one observed experimentally in twinned YBaCuO monocrystals by small-angle neutron scattering [31] and scanning tunnelling microscopy [9].

If we search for the solution of equation (6) as a linear combination of harmonics $e^{iq_x x}\hat{G}(q_x, y)$, the periodic functions f and $\boldsymbol{V}_s$ will be responsible for the interaction of the harmonics with q_x and $q_x + nb_{1x}$. As we see below, for $\varepsilon < 0.5\pi\Delta_0\xi/a$ the wave functions $\hat{G}(q_x, y)$ and $\hat{G}(q_x + nb_{1x}, y)$ do not overlap in the y-direction and, consequently, their interaction is negligible. In this case the momentum component q_x is a good quantum number and one can replace the exact periodic potential (7) in equation (6) with the effective potential averaged in the x-direction. The equation for $\hat{G}(q_x, y)$ reads

$$\xi\hat{\sigma}_z\left(q_x - \frac{\pi H y}{\phi_0}\right)\hat{G} - \frac{\mathrm{i}}{k_F}\hat{\sigma}_x\frac{\partial\hat{G}}{\partial y} + \frac{\pi\xi\sigma}{2R_y}\Phi\left(\frac{y}{R_y}\right)(1+\hat{\sigma}_z)\hat{G} = \frac{\varepsilon}{\Delta_0}\hat{G} \tag{8}$$

where $\Phi(z) = 2z - (2m+1)$ for $m < z < m+1$, m is an integer, and R_y (R_x) is the distance between the lines parallel to the x- (y-) axis and passing through the vortex centres. For type I (II) lattices we have $R_x = a$, $R_y = \sigma a$ ($R_x = a/2$, $R_y = \sigma a$). We omitted here the small corrections of the order ξ/a, which are connected with the suppression of the order parameter f in vortex cores. It is convenient to introduce $\hat{F} = (\hat{\sigma}_x + \hat{\sigma}_z)\hat{G}/2$ and the dimensionless values $z = y/R_y$, $Q = q_x R_y/(\pi\sigma)$, $E = \varepsilon/\varepsilon_y^*$, where $\varepsilon_y^* = \pi\Delta_0\xi\sigma/R_y$. At the mth interval ($m < z < m+1$) the equation for $\hat{F}$ reads

$$-\mathrm{i}\lambda\hat{\sigma}_z\frac{\partial\hat{F}}{\partial z} + \left(\frac{1}{2}\Phi(z) - E\right)\hat{F} + q_m\hat{\sigma}_x\hat{F} = 0 \tag{9}$$

where $q_m = Q - m - 1/2$ and $\lambda = (\pi\sigma k_F\xi)^{-1}$ is a dimensionless wavelength. A procedure analogous to the one described above can be carried out for the gap node at the point $\boldsymbol{k}_2 = (0, k_F)$. Taking the gauge $\boldsymbol{A} = -Hx\boldsymbol{y}_0$ and introducing

$$\hat{g} = e^{iq_y y}(\hat{\sigma}_x + \hat{\sigma}_z)\hat{F}^* \qquad z = -x/R_x \qquad q_y = \pi Q H R_x/\phi_0$$
$$\varepsilon = E\varepsilon_x^* \qquad \varepsilon_x^* = \pi\Delta_0\xi H R_x/\phi_0 \qquad \lambda^{-1} = \pi k_F\xi H R_x^2/\phi_0$$

one obtains equation (9). Due to the symmetry of the BdG equations, the solutions $U_{3,4}$, $V_{3,4}$, $\varepsilon_{3,4}$ for two other gap nodes at the points $\boldsymbol{k}_3 = (-k_F, 0)$ and $\boldsymbol{k}_4 = (0, -k_F)$ can be found by using the simple transformation $U_{3,4} \to V_{1,2}^*$, $V_{3,4} \to -U_{1,2}^*$, $\varepsilon_{3,4} \to -\varepsilon_{1,2}$.

The important point is that a set of eigenvalues corresponding to a certain momentum Q coincides with that for the momentum $Q+1$. Such a periodicity of the energy spectrum is a consequence of the periodicity of the potential $\Phi(z)$, as can be proved exactly from equation (9). Thus, to analyse the spectrum one can consider just the Q-values in the 1D Brillouin zone $-1/2 < Q < 1/2$. It may be useful to note that inside the mth interval the equations (9) are equivalent to the ones describing the interband tunnelling [32] or the one-dimensional (1D) motion of a Dirac particle in a uniform electric field, and can be solved exactly:

$$\hat{F} = \begin{pmatrix} c_1 D_{-\mathrm{i}\mu-1}(\tau) + c_2 D_{-\mathrm{i}\mu-1}(-\tau) \\ \mathrm{sgn}(Q-m-1/2)\sqrt{\mathrm{i}/\mu}(-c_1 D_{-\mathrm{i}\mu}(\tau) + c_2 D_{-\mathrm{i}\mu}(-\tau)) \end{pmatrix} \tag{10}$$

Here

$$\tau = \frac{2}{\mathrm{i}\lambda}(z - m - 1/2 - E) \qquad \mu = q_m^2/(2\lambda)$$

and $D_{-\mathrm{i}\mu-1}(\tau)$ and $D_{-\mathrm{i}\mu}(\tau)$ are the parabolic cylinder functions [33]. To obtain the energy spectrum one should match these solutions at points $z = m$ and obtain the system of two equations for c_1 and c_2. The solvability condition for this system results in the quantization rule. This procedure may be substantially simplified using the usual 1D quasiclassical approach which is valid for $\lambda \ll 1$. This condition is easily met for rather large $k_F\xi$-values, if the σ-parameter is not extremely large or small. Here we summarize the most important properties

of quasiclassical wave functions and energy spectrum, which are discussed in more detail in appendix A. The quasiparticle wave functions are localized in classically allowed (CA) regions which shift in the z-direction with a change in the Q-value. The discontinuities in $\Phi(z)$ at $z = m$ play the role of potential walls, and for rather low energies ($|E| < 1/2$) the dimension δz of each CA region does not exceed the distance between these walls (i.e. $\delta z < 1$). The classical motion at the mth interval is allowed provided that the condition $|Q - m - 1/2| < 1/2 + |E|$ is fulfilled. Inside this interval a linear increase in the $\Phi(z)$ potential results in the appearance of two turning points ($z_{1m} = m + 1/2 + E - |q_m|$ and $z_{2m} = m + 1/2 + E + |q_m|$). As a consequence, classical quasiparticles are locked in the following intervals: (i) $m < z < z_{1m}$ (region A); (ii) $z_{2m} < z < m + 1$ (region B). Using the Bohr–Sommerfeld quantization rule one obtains two sets of energy branches: $E_{\mathrm{A}}(N_{\mathrm{A}}, Q, m)$ and $E_{\mathrm{B}}(N_{\mathrm{B}}, Q, m)$ (see (A.5)).

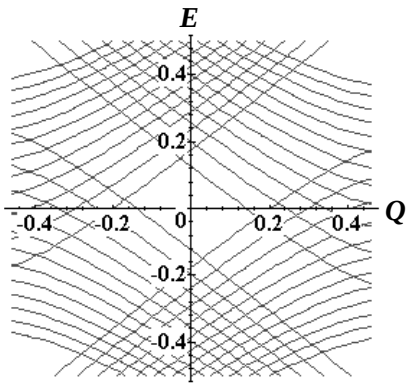

Figure 1. The energy branches in the first Brillouin zone for $\lambda = 0.01$.

In figure 1 we display these energy branches in the first Brillouin zone for the particular case of $\lambda = 0.01$. Near the points of intersection of the energy branches (A.5) in the E–Q plane one should take account of the splitting of energy levels, resulting from the quasiparticle tunnelling through classically forbidden regions. As a result, we obtain a set of narrow bands separated by energy gaps. The effect of tunnelling (and, therefore, energy splitting) is exponentially small, if the characteristic length of the wave-function decay in a classically forbidden region is much smaller than the dimension of this region. In the opposite case the effect of tunnelling is fundamental. In particular, we cannot neglect the tunnelling between the regions A and B for Q close to the Brillouin-zone boundaries, when the distance between the turning points z_{1m} and z_{2m} becomes comparable to the characteristic decay length $\sqrt{\lambda}$ in the region $z_{1m} < z < z_{2m}$. To analyse this limit we start from the exact solution (10) and replace the parabolic cylinder functions by the corresponding asymptotic expressions which are valid far from the turning points. Thus, if the turning points z_{1m} and z_{2m} are not too close to the m-interval boundaries ($z_{1m} - m \gg |q_m|, m + 1 - z_{2m} \gg |q_m|$) and the distance $z_{2m} - z_{1m}$ is rather small ($|q_m| \ll \sqrt{\lambda}$), the quantization rule takes the following form:

$$E \simeq E_{0N} + \sqrt{\pi\lambda} q_m (-1)^N \sin\left(\beta + \frac{E_{0N}^2}{4\lambda} - \frac{q_m^2}{2\lambda} \ln \frac{(1/4 - E_{0N}^2)}{\lambda}\right) \tag{11}$$

where

$$E_{0N} = \pi N \lambda + \lambda(\alpha_{\mathrm{A}} - \alpha_{\mathrm{B}})/2$$
$$\beta = \frac{\pi}{4} + \frac{1}{4\lambda} - \frac{\alpha_{\mathrm{A}} + \alpha_{\mathrm{B}}}{2}$$

where $N \in \mathbb{Z}$. The spectrum appears to be equidistant only at the Brillouin-zone boundaries ($Q = \pm 1/2$) and the distance between the energy levels depends strongly on the vortex lattice geometry.

One can see that for rather low energies ($|E| < 1/2$) the CA regions corresponding to the values Q and $Q + 2n$ do not overlap. In this case the interaction of the harmonics with q_x and $q_x + nb_{1x}$ will be exponentially small due to the exponential decay of the wave function in classically forbidden regions. For $|E| > 1/2$ the dimension of the CA region may exceed the intervortex distance, and the interaction of the overlapping harmonics $\hat{G}(q_x, y)$ and $\hat{G}(q_x + nb_{1x}, y)$ cannot be neglected. Thus, our procedure based on the averaging of the superfluid velocity in the x-direction is correct only for low energies $|E| < 1/2$, when the solutions are essentially localized in the y-direction on a scale determined by the intervortex distance. Using the solution of equation (9) given above, we obtain four sets of eigenfunctions and eigenvalues associated with four gap nodes. The range of validity of our approach is restricted by the condition $\varepsilon < 0.5 \min[\varepsilon_x^*, \varepsilon_y^*]$, where $\varepsilon_x^* \sim \Delta_0 \xi / R_x$ and $\varepsilon_y^* \sim \Delta_0 \xi / R_y$.

4. The density of states

The quantization of the low-energy spectrum should result in oscillatory behaviour of the DOS as a function of energy with the characteristic energy scales of orders given by

$$\delta\varepsilon_1 \sim \Delta_0 \sqrt{\hbar\omega_c/(\sigma E_F)}$$
$$\delta\varepsilon_2 \sim \Delta_0 \sqrt{\hbar\omega_c \sigma / E_F}$$

and, therefore, we unfortunately cannot explain a peak with a large energy gap $\lesssim \Delta_0$ observed experimentally at the vortex centres in YBaCuO [9]. The simplest way to analyse the local DOS $N(\varepsilon, x, y)$ in the low-energy regime is to neglect the oscillations and assume $N_{\mathrm{A,B}}$ to be a continuous variable (more detailed study is left as a future problem). In other words, for each gap node we consider the generalization of the usual semiclassical approach (see, e.g., [3]), taking account of the Doppler shift of the quasiparticle energy caused by the $\boldsymbol{V}_s$-field averaged in the gap node direction. We sum up the contributions from four gap nodes and obtain

$$N = \frac{\pi H \xi N_F}{4\phi_0} \left(R_x f\left(\frac{x}{R_x}, \frac{\varepsilon}{\varepsilon_x^*} \right) + R_y f\left(\frac{y}{R_y}, \frac{\varepsilon}{\varepsilon_y^*} \right) \right) \tag{12}$$

where

$$f(z, \tilde{\varepsilon}) = |\Phi(z)/2 - \tilde{\varepsilon}| + |\Phi(z)/2 + \tilde{\varepsilon}|$$

where N_F is the density of states at the Fermi level in a normal state.

Contour plots of the function

$$\nu = N N_F^{-1} \sqrt{32 H_{c2}/(\pi H)}$$

for the rectangular lattice with $\sigma = 2$ and for the hexagonal lattice with $\sigma = \sqrt{3}/2$ are shown in figures 2 and 3, respectively. The peaks in the local DOS ($\nu = \nu_{max}$) occur at the points $\boldsymbol{r}_{max} = (nR_x, mR_y)$ (n, m are integers) of intersection of lines parallel to the x- and y-axes and passing through the vortex centres. The interesting fact is that for type II lattices these peaks do not only appear at vortex centres, while for rectangular lattices (type I) the coordinates of all peaks coincide with the vortex positions. For $\varepsilon = 0$ the DOS vanishes at the points $\boldsymbol{r}_{min} = \boldsymbol{r}_{max} + (R_x/2, R_y/2)$. In the vicinity of each vortex centre $(\bar{x}, \bar{y})$ the local DOS exhibits a fourfold symmetry in analogy to the case of a single isolated vortex [16, 17, 21] and decreases linearly with increase of the distances $|x - \bar{x}|$ and $|y - \bar{y}|$ from the vortex centre (in

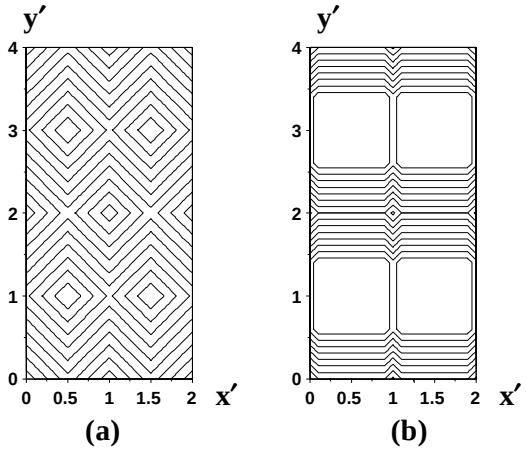

Figure 2. Contour plots of the normalized local DOS $\nu(\boldsymbol{r} = a\boldsymbol{r}')$ for the rectangular lattice with $\sigma = 2$. The ν-value changes from ν_{min} (at the points $\boldsymbol{r}'_{min} = \boldsymbol{r}'_{max} + (0.5, 1)$) to ν_{max} (at $\boldsymbol{r}'_{max} = (n, 2m)$). (a) $\varepsilon = 0$, $\nu_{min} = 0$, $\nu_{max} = 2.2$. (b) $\varepsilon = 0.2\varepsilon_y^*$, $\nu_{min} = 1.1$, $\nu_{max} = 2.2$.

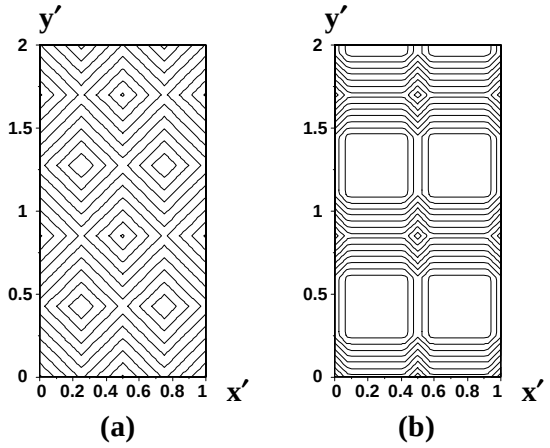

Figure 3. Contour plots of the normalized local DOS $\nu(\boldsymbol{r} = a\boldsymbol{r}')$ for the hexagonal lattice with $\sigma = 3^{1/2}/2$. The ν-value changes from ν_{min} (at the points $\boldsymbol{r}'_{min} = \boldsymbol{r}'_{max} + (0.25, \sigma/2)$) to ν_{max} (at $\boldsymbol{r}'_{max} = (n/2, \sigma m)$). (a) $\varepsilon = 0$, $\nu_{min} = 0$, $\nu_{max} = 1.6$. (b) $\varepsilon = 0.2\varepsilon_y^*$, $\nu_{min} = 0.7$, $\nu_{max} = 1.5$.

contrast to the $((x - \bar{x})^2 + (y - \bar{y})^2)^{-1/2}$ divergence resulting from the semiclassical approach based on equation (1)). The spatially averaged DOS has the form

$$\langle N \rangle = \frac{N_F}{8}\sqrt{\frac{\pi H}{2H_{c2}}}h(\sigma)\left(1 + \frac{4\varepsilon^2\phi_0 R_y}{\pi^2\xi^2\Delta_0^2 H\sigma R_x}\right) \tag{13}$$

where $h(\sigma) = \sigma^{1/2} + \sigma^{-1/2}$ ($h(\sigma) = \sigma^{1/2} + 0.5\sigma^{-1/2}$) for the type I (II) lattice. If we assume the parameter σ to be field independent, then the magnetic field dependence of the residual DOS (at $\varepsilon = 0$) follows the square-root behaviour which was first predicted in [3]. Deviations from this behaviour may appear if the vortex lattice structure and, hence, the σ-value change with the magnetic field increase (see [25, 26, 28–30]) and, probably, they are relevant to the interpretation of specific heat [6–8] and thermal conductivity [34, 35] measurements for high-

T_c compounds. Note that to make realistic predictions for experiments one should, certainly, take account of the disorder effects [4, 5].

5. Conclusions

In summary, we have described the distinctive features of the low-lying quasiparticle states in the vortex lattices in d-wave systems. The periodic superfluid velocity field is shown to induce the band structure in the low-energy part of the spectrum. This band structure and corresponding eigenfunctions have been analysed for both rectangular and centred rectangular flux lattices tilted by $\pi/4$ from the a-axis. We also believe that our results will be qualitatively valid for a larger class of flux lattices, including, probably, the ones observed experimentally in twinned YBaCuO monocrystals [9, 31]. Contrary to the case for s-wave superconductivity, the spectrum quantization in d-wave systems is not connected with vortex core regions. For the quasiparticle states associated with each gap node there exist two regimes with the crossover parameter $\varepsilon R_i/(\Delta_0\xi)$ ($i = x$ and $i = y$ for the gap nodes at $\boldsymbol{k}_{2,4}$ and $\boldsymbol{k}_{1,3}$, respectively):

(a) for the low-energy regime the spectrum has a band structure, and the wave functions are extended in the gap node direction and localized in the perpendicular one on a scale determined by the intervortex distance;
(b) for the high-energy regime the spectrum is continuous, the eigenfunctions are extended in both directions, and our approximate solution based on the averaging of the superfluid velocity in the gap node direction is no longer valid.

The characteristic energy ε of the excitations coming into play at finite temperatures is of the order of T and, consequently, for thermodynamic and transport quantities one can expect different regimes with the crossover parameters $TR_x/(\Delta_0\xi)$, $TR_y/(\Delta_0\xi)$. Taking the case where

$$R_x \sim R_y \sim \sqrt{\phi_0/H}$$

we obtain the crossover parameter introduced previously in [10, 12, 23]. The resulting peculiarities of the local DOS in the low-energy regime are shown to be strongly influenced by the vortex lattice geometry. The unusual behaviour of the DOS discussed above can be probed by specific heat and STM measurements, and could provide additional arguments in favour of d-wave pairing in high-T_c superconductors. The present study provides a starting point for the analysis of static and dynamic properties of the mixed state in various d-wave systems, including, probably, high-T_c copper oxides. For this purpose the approach developed above should be generalized to describe the quasiparticle states for arbitrary lattice orientations with respect to the crystal axes.

Acknowledgments

It is my pleasure to thank Dr I D Tokman, Dr M Franz, and Professor Z Tešanović for very useful discussions of the issues considered in this article. This work was supported, in part, by the Russian Foundation for Fundamental Research (Grant No 97-02-17437).

Appendix A

Following the usual quasiclassical procedure, we substitute $\hat{F} \propto \exp(\mathrm{i}S(z))$ in equation (9) and obtain the classically allowed (CA) regions (where the function S is real): $|\Phi(z)/2 - E| > |q_m|$.

These regions shift in the z-direction with a change in the Q-value, and the quasiparticle motion at the mth interval is classically allowed only for $|q_m| < 1/2 + |E|$. In the low-energy limit $|E| < 1/2$, the CA regions at this interval cannot appear for $|q_m| > 1$. Let us now consider the domain $|q_m| < 1$ and continue with the calculation of quasiclassical wave functions and energy levels corresponding to the quasiparticle motion at the mth interval which contains two CA regions: (i) $-1/2 < z-m-1/2 < E-|q_m|$ (region A) and (ii) $E+|q_m| < z-m-1/2 < 1/2$ (region B). Note that the region A (B) exists if the turning point $z_{1m} = m + 1/2 + E - |q_m|$ ($z_{2m} = m + 1/2 + E + |q_m|$) belongs to the mth interval. The wave functions and quantization rules for regions A and B can be written as follows:

$$\hat{F}_{\mathrm{A,B}} = \frac{C_{\mathrm{A,B}}}{(t^2-q_m^2)^{1/4}}\left(\frac{\exp(\mathrm{i}S_{\mathrm{A,B}})}{|t+\sqrt{t^2-q_m^2}|^{1/2}}\begin{pmatrix}-q_m\\ t+\sqrt{t^2-q_m^2}\end{pmatrix} + \frac{\exp(-\mathrm{i}S_{\mathrm{A,B}})}{|t-\sqrt{t^2-q_m^2}|^{1/2}}\begin{pmatrix}-q_m\\ t-\sqrt{t^2-q_m^2}\end{pmatrix}\right) \tag{A.1}$$

$$S_{\mathrm{A,B}} = \frac{1}{\lambda}\int_{\mp|q_m|}^{t}\sqrt{s^2-q_m^2}\,\mathrm{d}s \pm \frac{\pi}{4}\int_{|q_m|}^{1/2\pm E}\sqrt{t^2-q_m^2}\,\mathrm{d}t = \pi\lambda(N_{\mathrm{A,B}}+\gamma_{\mathrm{A,B}}(q_m)) \tag{A.2}$$

where $t = z - m - 1/2 - E$, and $N_{\mathrm{A,B}}$ is an integer. The $\gamma_{\mathrm{A,B}}$-values are of the order of unity and are determined by the matching of the expression (A.1) with the exponentially decaying solutions in classically forbidden regions at the $(m-1)$th and $(m+1)$th intervals. This matching procedure results in the following boundary conditions for the wave function $\hat{F} = (F_1, F_2)$:

$$\left.\frac{F_2}{F_1}\right|_{z=m} = \exp(\mathrm{i}\alpha_{\mathrm{A}}) \qquad \cos\alpha_{\mathrm{A}} = \frac{E-1/2}{Q-m+1/2} \tag{A.3}$$

$$\left.\frac{F_2}{F_1}\right|_{z=m+1} = \exp(\mathrm{i}\alpha_{\mathrm{B}}) \qquad \cos\alpha_{\mathrm{B}} = \frac{E+1/2}{Q-m-3/2}. \tag{A.4}$$

Evaluating the integral in the l.h.s. of equation (A.2), one obtains

$$\left(\frac{1}{2}\pm E_{\mathrm{A,B}}\right)\sqrt{\left(\frac{1}{2}\pm E_{\mathrm{A,B}}\right)^2-q_m^2} - q_m^2\cosh^{-1}\left(\frac{\frac{1}{2}\pm E_{\mathrm{A,B}}}{|q_m|}\right) = 2\pi\lambda(N_{\mathrm{A,B}}+\gamma_{\mathrm{A,B}}). \tag{A.5}$$

Near the first Brillouin-zone boundary $|Q - 1/2| \ll 1/2 \pm E$, the spectrum has the following simple form:

$$E_{\mathrm{A,B}}\Big|_{m=0} \simeq \mp\frac{1}{2} \pm \sqrt{2\pi\lambda(N_{\mathrm{A,B}}+\gamma_{\mathrm{A,B}})} \pm \frac{(Q-1/2)^2}{2\sqrt{2\pi\lambda(N_{\mathrm{A,B}}+\gamma_{\mathrm{A,B}})}}\ln\frac{\sqrt{2\pi\lambda(N_{\mathrm{A,B}}+\gamma_{\mathrm{A,B}})}}{|Q-1/2|}. \tag{A.6}$$

Note added in proof. After submission of this paper I learned that M Franz and Z Tešanović [36] have obtained a numerical solution describing the band spectrum for a square lattice (type II, $\sigma = 0.5$). For rather large anisotropy of the spectrum (2), the numerical solution [36] appears to be in good agreement with our analytical results.

References

[1] Annett J, Goldenfeld N and Leggett A J 1996 *Physical Properties of High Temperature Superconductors* vol 5, ed D M Ginsberg (Singapore: World Scientific)

[2] Caroli C, P G de Gennes and Matricon J 1964 *Phys. Lett.* **9** 307

[3] Volovik G E 1993 *JETP Lett.* **58** 469

[4] Barash Yu S, Mineev V P and Svidzinskii A A 1997 *JETP Lett.* **65** 638

[5] Kübert C and Hirschfeld P J 1998 *Solid State Commun.* **105** 459

[6] Moler K A, Baar D J, Urbach J S, Liang R, Hardy W N and Kapitulnik A 1994 *Phys. Rev. Lett.* **73** 2744
[7] Moler K A, Sisson D L, Urbach J S, Beasley M R and Kapitulnik A 1997 *Phys. Rev.* B **55** 3954
[8] Revaz R A, Junod A, Mirmelstein A, Erb A, Genoud J Y, Triscone G and Muller J 1996 *Czech J. Phys. Suppl.* S3 **46** 1205
[9] Maggio-Aprile I, Renner Ch, Erb A, Walker E and Fisher Ø 1995 *Phys. Rev. Lett.* **75** 2754
[10] Kopnin N B and Volovik G E 1996 *JETP Lett.* **64** 690
[11] Kopnin N B and Volovik G E 1997 *Phys. Rev. Lett.* **79** 1377
[12] Kopnin N B 1998 *Phys. Rev.* B **57** 11 775
[13] Makhlin Yu G 1997 *Phys. Rev.* B **56** 11 872
[14] Simon S H and Lee P A 1997 *Phys. Rev. Lett.* **78** 1548
[15] Franz M and Tešanović Z 1998 *Phys. Rev. Lett.* **80** 4763
[16] Schopohl N and Maki K 1995 *Phys. Rev.* B **52** 490
[17] Ichioka M, Hayashi N, Enomoto N and Machida K 1996 *Phys. Rev.* B **53** 15 316
[18] Gor'kov L P and Schrieffer J R 1998 *Phys. Rev. Lett.* **80** 3360
[19] Soininen P I, Kallin C and Berlinsky A J 1994 *Phys. Rev.* B **50** 13 883
[20] Wang Y and MacDonald A H 1995 *Phys. Rev.* B **52** R3876
[21] Morita Y, Kohmoto M and Maki K 1997 *Preprint* cond-mat/9706118
[22] Bruder C 1990 *Phys. Rev.* B **41** 4017
[23] Volovik G E and Kopnin N B 1997 *Phys. Rev. Lett.* **78** 5028
[24] Simon S H and Lee P A 1997 *Phys. Rev. Lett.* **78** 5029
[25] Franz M, Affleck I and Amin M H S 1997 *Phys. Rev. Lett.* **79** 1555
[26] Amin M H S, Affleck I and Franz M 1998 *Phys. Rev.* B **58** 5848
[27] Won H and Maki K 1996 *Phys. Rev.* B **53** 5927
[28] Shiraishi J, Kohmoto M and Maki K 1999 *Phys. Rev.* B **59** 4497
[29] Shiraishi J, Kohmoto M and Maki K 1998 *Preprint* cond-mat/9802067
[30] Ichioka M, Enomoto N and Machida K 1997 *Preprint* cond-mat/9704147
[31] Keimer B, Shin W Y, Erwin R W, Lynn J W, Dogan F and Aksay I A 1994 *Phys. Rev. Lett.* **73** 3459
[32] Kane E O and Blount E I 1969 *Tunnelling Phenomena in Solids* ed E Burstein and S Lundqvist (New York: Plenum)
[33] Whittaker E T and Watson G N 1947 *Modern Analysis* (Cambridge: Cambridge University Press)
[34] Krishana K, Ong N P, Li Q, Gu G D and Koshizuka 1997 *Science* **277** 83
[35] Aubin H, Behnia K, Ooi S and Tamegai T 1999 *Phys. Rev. Lett.* **82** 624
[36] Franz M and Tešanović Z 1999 *Preprint* cond-mat/9903152